Food Chemistry xxx (xxxx) xxx

Contents lists available at ScienceDirect

Food Chemistry

journal homepage: www.elsevier.com/locate/foodchem

Elucidation of the non-volatile fingerprint in oven headspace vapor from bread roll baking by ultra-high resolution mass spectrometry

Leopold Weidner [a,b], Yingfei Yan [b], Daniel Hemmler [a,b], Michael Rychlik [a], Philippe Schmitt-Kopplin [a,b,*]

[a] Comprehensive Foodomics Platform, Chair of Analytical Food Chemistry, TUM School of Life Sciences, Technical University of Munich, Maximus-von-Imhof-Forum 2, 85354 Freising, Germany

[b] Helmholtz Zentrum Muenchen, Analytical BioGeoChemistry, Ingolstaedter Landstr. 1, 85764 Neuherberg, Germany

ARTICLE INFO

Keywords:
Headspace sampling
Response surface methodology
Maillard reaction
FT-ICR-MS
Foodomics
Wheat bread

Chemical compounds:
Maltosine (PubChem CID: 71749894)

ABSTRACT

Untargeted research on vapor arising during the thermal processing of food has so far focused on volatile aroma compounds. In this study, we present an oven atmosphere sampling strategy to trap headspace aerosols along with semi- and non-volatile molecules liberated during the baking of wheat bread rolls. The collected vapor condensate was analyzed for its molecular fingerprinting using direct infusion ultra-high resolution mass spectrometry. We detected up to 4,700 molecular species in a vapor sample from bread rolls baked at 230 °C for 15 min. Beyond the global profiling of the underlying matrix, our method can follow complex reaction cascades during the baking process, such as the formation of advanced glycation end-products like maltosine through the interface of trapped vapor. Further, process parameters such as baking temperature and duration were used to model the dynamic liberation of molecules to the oven atmosphere by a response surface methodology approach.

1. Introduction

During production of cereal products, baking of the dough represents the final process step before human consumption. By the application of heat, a multitude of chemical reactions and transformations is triggered inducing huge changes to the dough. The exact elucidation of chemical transformations induced by thermal processing of bakery products thereby is of fundamental interest in analytical food chemistry. During every heating process water rises from the matrix to the headspace of the processing vessel. In 1952, Pence introduced the novel concept of studying this vapor by the principle of physically condensing vapor from bread baking as an additional and easily accessible source of information about processes occurring during cooking. Collected condensate was analyzed by thin-layer chromatography, fractional distillation and identification of functional groups (Pence, 1952). Later, Lee et al. fortified bread dough with ^{14}C labeled sucrose and studied its dispersion in oven vapor by the same sampling approach (Lee & Chen, 1966). These studies were the first untargeted investigations of oven vapor. As analytical food chemistry advanced in the following years, the focus on research of processed food has been on the matrix itself. In the few cases when its headspace was studied during processing, most protocols focused on the analysis of volatile molecules contained in the vapor. In particular, solid-phase microextraction (SPME) coupled to gas chromatography with mass spectrometric detection (GC–MS) (Rega, Guerard, Delarue, Maire, & Giampaoli, 2009; Rochat & Chaintreau, 2005) and proton transfer reaction (PTR) MS (Pico, Khomenko, Capozzi, Navarini, & Biasioli, 2020; Wieland et al., 2012) were used to study aroma active compounds evolving during thermal processing. Both approaches focus on the analysis of volatile compounds. PTR-MS is a direct infusion technique and as such capable of analyzing the oven headspace in real time during baking. In contrast, analytes can be absorbed on a SPME fiber online during baking, but desorption and analysis of these samples by GC–MS is performed after the baking experiment. Nevertheless, it benefits from chromatographical separation before mass spectrometric detection. As Pence already demonstrated that oven vapor is composed of various substance classes beyond volatiles, there currently seems to be a methodological lack of holistic investigations about semi- and non-volatile molecules within this matrix. Based on the original study from Pence, we intend to develop an advanced vapor sampling protocol and to apply it by sampling vapor released from commercial wheat bread

* Corresponding author at: Comprehensive Foodomics Platform, Chair of Analytical Food Chemistry, TUM School of Life Sciences, Technical University of Munich, Maximus-von-Imhof-Forum 2, 85354 Freising, Germany.
E-mail addresses: leopold.weidner@tum.de (L. Weidner), schmitt-kopplin@tum.de (P. Schmitt-Kopplin).

https://doi.org/10.1016/j.foodchem.2021.131618
Received 22 June 2021; Received in revised form 29 October 2021; Accepted 11 November 2021
Available online 17 November 2021

rolls. The collected condensate sample shall be analyzed by direct injection analysis Fourier-transform ion cyclotron resonance mass spectrometry (DIA-FT-ICR-MS), the up-to-date most powerful analytical platform for in-depth metabolomic profiling of complex products (Hertkorn et al., 2008; Marshall, Hendrickson, & Jackson, 1998; Marshall & Rodgers, 2004). Ultra-high resolution mass spectrometry datasets from FT-ICR-MS studies already gave insights into the molecular complexity of foodstuffs like wine, whiskey and beer (Pieczonka, Lucio, Rychlik, & Schmitt-Kopplin, 2020; Roullier-Gall et al., 2014; 2018). Similar to the SPME approach developed by Rega et al. our approach comprises an atline-measurement strategy to fully take advantage of the benefits offered by FT-ICR-MS. In contrast to SPME and PTR techniques both focusing on volatiles, we aim to extend the knowledge about compounds contained in oven vapor to a broader range of analyte polarity and molecular weight by our research. We want to understand the release dynamics of compounds liberated to the oven headspace triggered by thermal causes and to further investigate the information about the underlying food reactome mediated by oven vapor. Based on the profiling, we developed a response surface methodology (RSM) in the second part of this work which permits us to monitor the presence of molecules in the oven headspace as a function of processing parameters such as baking temperature and duration.

2. Materials and methods

2.1. Materials

Ultra-pure water was supplied by a Milli-Q integral system (Merck, Darmstadt, Germany). Arginine (reagent grade, 98%) was purchased from Sigma Aldrich (Taufkirchen, Germany). Methanol (LC–MS grade) was obtained from Fisher Scientific (Schwerte, Germany); Ethanol (99%) was purchased from Brenntag (Essen, Germany) and dry ice pellets were purchased from Polar (Neustadt an der Donau, Germany).

2.2. Food samples

Wheat bread roll samples (approximately 65 g each) were purchased from an industrial bakery (Froneri, Nürnberg, Germany). Formulation as well as nutritional composition of the samples are documented in Supplementary Table 1. The doughs were risen, partially pre-baked and deep-frozen. Only the final baking phase, which is usually performed by the end-customer, was investigated during this study. Doughs were stored at –21 °C immediately until baking.

2.3. Baking of bread rolls:

All doughs were baked in a professional oven. Doughs were baked in the “hot-air” instrument-mode. Temperature and baking time ranged around a center point of 200 °C and 12 min, which was optimized for the utilized oven based on the manufacturer’s recommendations during pretests. The studied temperature and time values reached from 158 to 242 °C and from 7.8 to 16.2 min (see Supplementary Table 2). Humidity was set to 100%. A total of six doughs per experiment were baked on an ordinary metal sheet at the middle slot of the baking chamber and baked under a medium level of convection. Bread rolls were placed inside the oven after pre-heating and equilibration of the baking chamber. All baking events were performed in triplicate and in randomized order.

2.4. Oven vapor sampling:

The oven was daily cleaned and baked out at 300 °C prior to sampling. Void-runs were sampled on a daily basis to monitor possible contaminants in the background. A small glass tube connected to a hose made of polytetrafluoroethylene (PTFE) was inserted into the baking chamber through the sealing of the door. A negative pressure system was used to draw vapor and gases from the inside of the baking chamber towards a chilled condenser-apparatus. The condensate was collected in a round-bottomed flask (see Fig. 1 for a schematic drawing of the entire apparatus). Sample collection was performed cumulatively over the entire baking duration. The pump was operated at a constant speed of 1.3 L min^{-1}. Hose and condenser were rinsed with 5 mL of ultra-pure water after each baking experiment to collect remaining analytes. Samples were stored at –80 °C and consecutively lyophilized until complete dryness. Subsequently, residues were reconstituted in 200 µL of ultra-pure water. After incubating in an ultrasonic bath for 10 min, samples were centrifuged at 15,000 rpm for 15 min. Finally, the clear supernatant was diluted with methanol by a factor of 10 (*v/v*) prior to mass spectrometric analysis.

2.5. Direct infusion FT-ICR mass spectrometry data acquisition:

Ultra-high resolution mass spectra were acquired in direct flow injection mode on a solariX FT-ICR mass spectrometer equipped with a 12 T superconducting magnet (Bruker Daltonics, Bremen, Germany). The diluted samples were automatically injected by a PAL RTC system autosampler (CTC Analytics, Zwingen, Switzerland) at a constant flow rate of 2 µL min^{-1}. Electrospray ionization (ESI) was performed in negative ion mode using an APOLLO II ion source. Source parameters were set as follows: dry gas flow rate 4 L min^{-1} at 180 °C, nebulizer gas flow 2.2 bar (both nitrogen), capillary voltage 3600 V and spray shield voltage –500 V. Spectra were acquired with a time-domain of 4 megawords. Ions were accumulated for 0.4 s per scan and a total number of 200 scans from *m/z* 122 to *m/z* 1000 were accumulated per sample. External calibration of spectra was performed with ion clusters of arginine (5 ppm in methanol). The injection order of samples was completely randomized.

2.6. Processing of FT-ICR-MS data:

Raw spectra were preprocessed by Compass DataAnalysis 5.0 (Bruker Daltonics, Bremen, Germany). In addition to calibration of the instrument’s mass analyzer, internal calibration of spectra with a reference mass list was performed. The reference list was composed of ubiquitous masses like fatty acids on the one hand and of reliably identified masses specific for oven vapor on the other. Internal calibration and further data analysis were performed over a mass range from 122 Da to 600 Da. Ion signals with a signal-to-noise ratio of at least six were exported into mass lists. All further data post-processing and analysis steps were performed in R programming language (R Foundation for Statistical Computing, Vienna, Austria). Only singly charged ions were considered for analysis. Exported mass lists were consecutively aligned into a matrix consisting of averaged *m/z* values for every detected peak and corresponding intensity values for all samples. The mass list was cleaned up for side bands, heavy isotope peaks and ion-adducts (Kanawati, Bader, Wanczek, Li, & Schmitt-Kopplin, 2017).

Chloride adducts were converted to the corresponding $[M-H]^-$ ions. On average only one ^{34}S isotope peak was identified per analyzed sample; thus sulfur was assumed to play a minor role in the matrix. Assignment of molecular formulas was therefore restricted to the CHNO space. Based on a mass difference network analysis (Tziotis, Hertkorn, & Schmitt-Kopplin, 2011), molecular formulas for the remaining exact mass values were calculated and assigned to the matrix. Thereby, isobaric compounds cannot be distinguished, as direct flow injection techniques do not permit the separation of isomers. Only features which were present in at least two out of three sample replicates were considered for annotation and further analysis.

2.7. Response surface methodology:

To investigate the relative abundance of compounds released into the headspace during bread baking at different processing conditions, a fractional factorial experimental plan with a central composite compo-

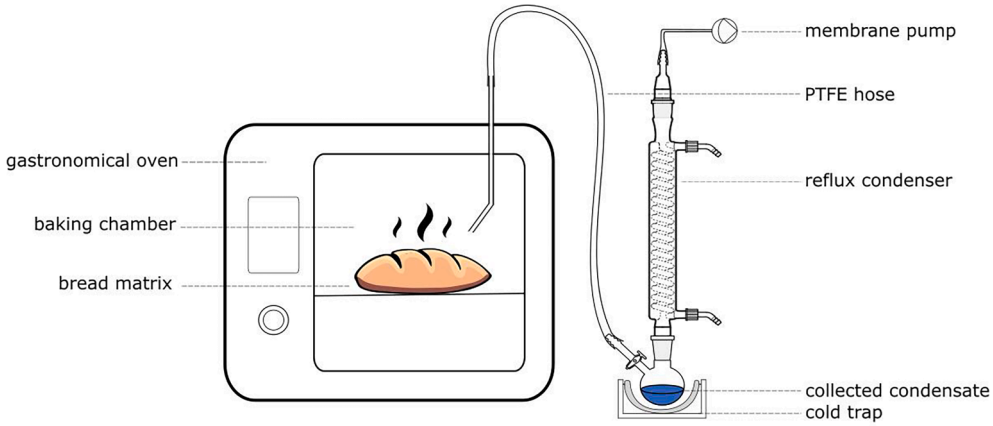

Fig. 1. Schematic drawing of the sampling apparatus. Oven vapor is drawn by a negative pressure system out of a baking chamber and condensed in a round bottom flask for later analysis.

nent was set up. Baking temperature and baking time were chosen as experimental factors to investigate. Their uncoded levels ranged from 158 to 242 °C and from 7.8 to 16.2 min, respectively. A total number of 21 factor combinations within these ranges were investigated. Information about coding of factor levels for all baking experiments is given in Supplementary Table 2. Prior to RSM analysis, missing values within the matrix were filled by a Random Forest (RF) imputation strategy (Stekhoven & Bühlmann, 2012). Subsequently, we performed response surface modelling for every feature in the matrix to describe its relative concentration in the headspace as a function of variable processing parameters. Initially, second order polynomial models (see equation (1)) were fitted to the feature's intensities acquired at different temperature (T) and time (t) pairings.

$$\widehat{Y} = \widehat{\beta_0} + \widehat{\beta_1}T + \widehat{\beta_2}t + \widehat{\beta_{12}}Tt + \widehat{\beta_{11}}T^2 + \widehat{\beta_{22}}t^2 \quad (1)$$

A full second order model consists of first order (FO), two way interaction (TWI) and pure quadratic (PQ) term parts. Variable selection and optimization of models were carried out based on comparative likelihood-ratio tests using the Akaike information criterion (AIC) (Akaike, 1974). The AIC was used in an automated script to estimate the prediction errors of every possible composition of a model by stepwise leave-one-out validation of single term parts. The model-version yielding the lowest prediction error, and thus the lowest AIC-score, was regarded as most accurate. Furthermore, only those models were accepted which had an adjusted $R^2 > 0.6$.

2.8. Validation of models

Baking processes at two further, randomly selected processing conditions were used to assess the prediction capacity of the calculated models. Precisely, a random number generator was used to create two temperature–time pairings within the covered factor ranges which are subsequently addressed as validation points (VP). Bread rolls were baked, sampled and analyzed at these points in triplicates similar to the 21 sample points. Intensities of features measured at the VP were not included in the calculations of the models. For each feature-specific model, the measured intensities at these VP were compared to the model's predicted values. Therefore, the standard deviation of a model's residues was calculated. Then, it was checked if the prediction of a model deviated less than two standard deviations from the actual intensity recorded in both VP samples. Only models which validly predicted both VP were regarded as resilient.

3. Results and discussion

3.1. Cold trapping steam from baking processes

We constructed a simple and robust sampling apparatus targeted for trapping oven vapor. A schematic drawing is shown in Fig. 1. The glass parts of the apparatus are easily accessible and permit careful cleaning between sampling runs to avoid carry-over. The glass tube introduced into the baking chamber as well as the attached PTFE hose were subject to relatively heavy pollution as they conducted the steam-assisted sample transfer and thus were exchanged on a regular basis. Although we did focus on one professional oven, the apparatus could be used to sample any other baking system with similar door sealings without the need of installing permanent modifications on the system. By operating the membrane pump at a constant speed of 1.3 L min^{-1} we conveyed between approximately 2 and 8 mL of condensate per baking experiment at a constant load of six bread rolls per experiment. With increasing baking temperature from 170 to 242 °C and baking duration from 9.0 to 16.2 min, the amount of collected liquid increased likewise.

Sample collection was performed cumulatively over the entire baking run and the full amount of collected liquid was used for analysis. The cooling bath and the reflux condenser were filled with ice water, at a temperature of 4 °C, to support condensation of the conducted steam and to preserve sample constitution prior to storing the sample at –80 °C. We additionally tested the option to cool the round-bottomed flask with a cold mixture consisting of ethanol and dry ice at –72 °C. Under this condition, the volume of the trapped condensate did not increase compared to cooling with wet ice in water, so we considered the latter as a sufficient cooling medium for our experiments. As the pumped steam warms up the cooling bath during sampling, colder trapping temperatures might nevertheless be beneficial and should be considered in the case of (i) very hot processing conditions, (ii) sampling large volumes of vapor, (iii) extensive sampling runs, (iv) targeted sampling of labile analytes or (v) targeted sampling of semi-volatile analytes. Recently, there have been advances in investigations about the volatile components of oven vapor (Ait Ameur, Rega, Giampaoli, Trystram, & Birlouez-Aragon, 2008; Rega et al., 2009). The referred authors applied a similar sampling procedure: they likewise pumped vapor out of the baking chamber of an oven towards a refrigerated extraction chamber. Analytes were therein adsorbed on solid-phase microextraction (SPME) fibers and subjected to gas chromatography analysis with various detection systems. However, during these studies the condensate which was still containing semi- and non-volatiles was discharged after SPME. The presented online SPME analysis yields excellent results in the monitoring of volatiles such as furfurals, short-chained aliphatic acids and aldehydes or pyrazines that evolve during the baking process. Further,

related analytical work on oven vapor was executed by proton transfer reaction PTR-MS (Pico et al., 2020; Wieland et al., 2012). In PTR-MS volatile organic compounds (VOC) are ionized by transferring a proton from H_3O^+ ions to analytes having a greater proton affinity than water. Whereas PTR-MS analysis of baking processes can be performed online and in real-time, it operates under the limitations of ionizing uniquely molecules with proton-accepting functionalities. FT-ICR-MS on the contrary is favored by using universal electro spray ionization which can be operated in positive and negative ion mode and performs versatile in the analysis of complex organic mixtures (Hertkorn et al., 2008). The findings based on PTR-MS and SPME-analysis of oven vapor strongly emphasize the opportunities offered by oven vapor sampling and encourage us to extend the field of research toward semi- and non-volatile compounds.

3.2. Molecular complexity of oven vapor during bread roll baking:

We obtained molecular fingerprints of oven vapor by electrospray (–) FT-ICR-MS with a primary interest on semi- and non-volatile molecules. After aligning mass lists and applying data pre-treatment filters, the matrix for the entire dataset of 63 collected condensate samples consisted of >6,700 features, each representing a monoisotopic mass signal. An original spectrum, as well as an example crop showing the distinct fingerprinting pattern of six bread rolls baked at 230 °C for 15 min are shown in Fig. 2a/**b**. In the 0.16 Da section, 33 ion signals (S/N > 6) were detected, already illustrating the high density of information contained in oven vapor. For this spectrum, a resolution of 740,000 at *m/z* 200 and of 410,000 at *m/z* 400 was achieved. The assignment of molecular formulas to the matrix was restricted to a ± 100 ppb error window. Of the assigned matrix, 77% of all annotated formulas could be found within -50 ppb < error < +50 ppb (see Fig. 1c). As opposed to the entire matrix, we detected a total of 4,738 annotated mass signals in the condensate collected from six bread rolls baked at 230 °C for 15 min. This refers to the final number of features after application of pre-filtering algorithms and replicate filtering. A second sample arising from six bread rolls baked for the same time but at 170 °C was determined to contain only 580 detectable features. Comparing all annotated ion signals in both samples, we observed a median molecular mass of 319 Da (170 °C, 15 min) opposed to 366 Da (230 °C, 15 min) under the analytical conditions applied (see points 2.4–2.6). Thus, increasing baking temperature by 60 °C triggers an eightfold change in feature number with significantly higher median molecular mass in the oven headspace (Wilcoxon Rank test, W = 1,817,740, $p \leq 0.0001$, $n = 5{,}318$ features).

We further observed a change in the chemical composition of the samples: whilst the 170 °C condensate showed a CHO:CHNO ratio of 0.7, the rate decreasing to 0.5 in the 230 °C sample. The inter-sample ratios of feature numbers assigned to the CHO, CHN_1O and CHN_3O roughly followed the eight-fold change of total feature numbers, whereas there are 17 times more compounds assigned to the CHN_2O space in oven vapor from bread rolls baked at 230 °C for 15 min. From both trends we conclude a favored entry of nitrogen into the CHO space by rising baking temperature (see Fig. 3e for visualization). Likewise, the evaluation of characteristic bulk descriptors such as double bond equivalents, aromaticity index and average H/C-rate altogether confirm a higher degree of unsaturation among features detected at higher baking temperatures. Variation of baking time was found to have less impact on the number of features, molecular mass and chemical composition than baking temperature. Next to these two samples, which we exemplarily discussed here, we conducted experiments at 19 further baking temperature-duration combinations for our RSM calculations. These vapor samples follow the same trends as discussed above (see Supplementary Fig. 1). The compositional differences between both samples are cross-plotted by Van-Krevelen and respective H/C- to *m/z*-plots (see Fig. 3a–d): Van-Krevelen plots are a versatile, graphical tool for the

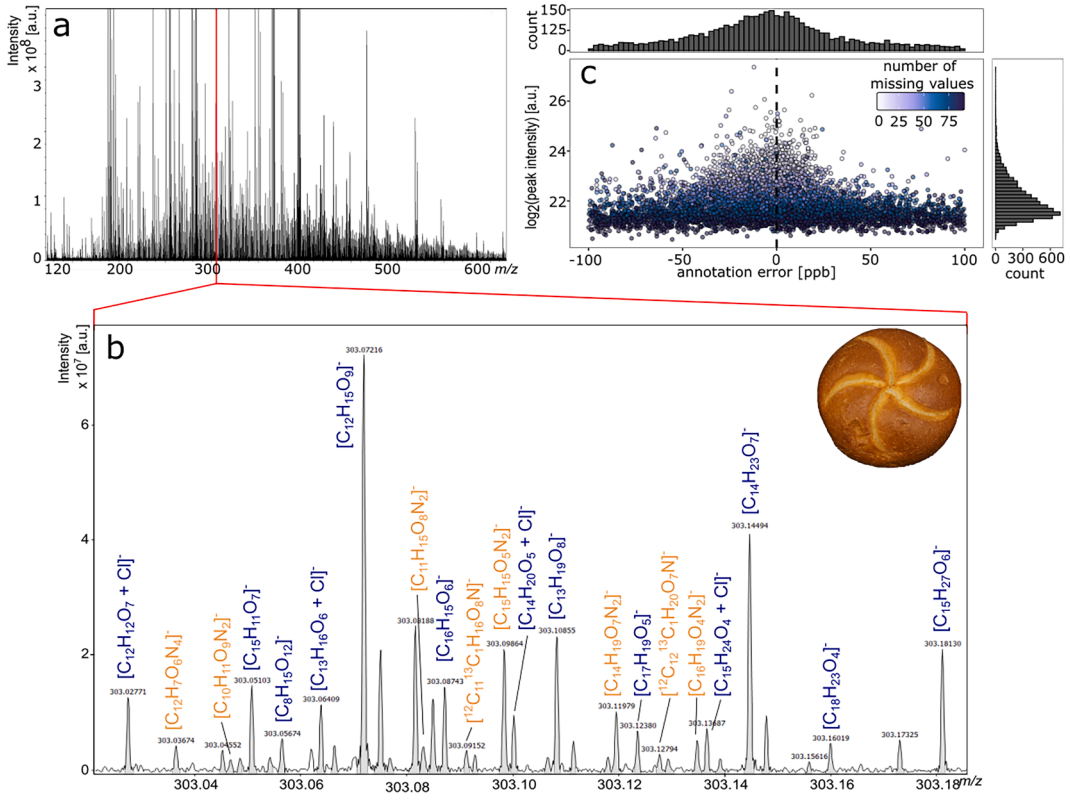

Fig. 2. **a** Complete FT-ICR-MS spectrum of a vapor sample from six bread rolls baked at 230 °C for 15 min. **b** We detected a total of 33 mass signals, of which two are ^{13}C heavy isotope peaks, in a 160 mDa crop of the spectrum at *m/z* 303. **c** Annotation error plot of the aligned matrix with histograms showing their distributions. A total of 77% of all annotated formulas range within the sub 50 ppb range. Point color refers to the detection frequency of the feature.

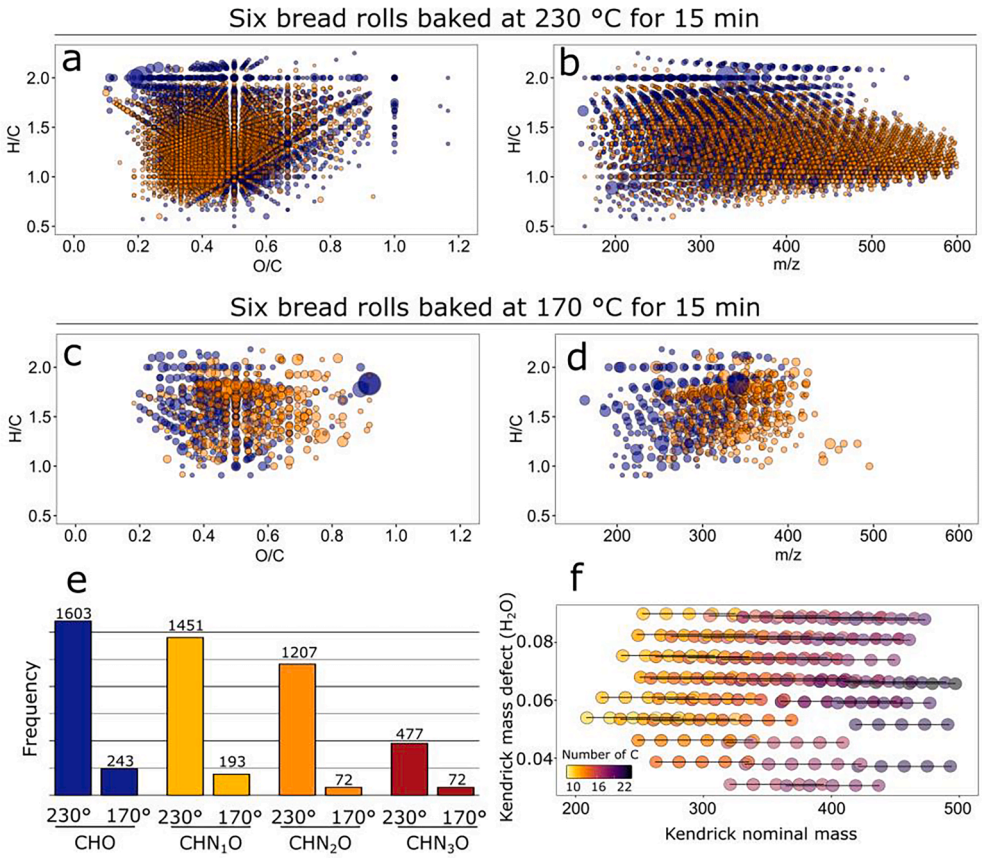

Fig. 3. Compositional overviews of oven vapor by Van Krevelen plots and H/C to *m/z* plots of six bread rolls each baked at 230 °C for 15 min (**a**,**b**) and at 170 °C for 15 min (**c**, **d**) (point size proportional to feature intensity). **e** Composition of chemical spaces in both samples. **f** Visualization of dehydration transitions by normalizing IUPAC mass to a water Kendrick Mass scale (*m/z* * 18/18.010565). Series with the same Kendrick Mass Defect and same number of Carbon atoms are connected by straight lines. Only series with at least five consecutive water mass difference increments are shown.

visualization of untargeted ultrahigh-resolution mass spectrometric datasets (Hertkorn et al., 2008; Kim, Kramer, & Hatcher, 2003). Cross-plotting hydrogen:carbon (H/C) and oxygen:carbon (O/C) ratios of all annotated molecular formulas helps illustrating and characterizing the chemical diversity of the vapor samples by associating detected ions with compound classes. Further, straight lines connecting multiple points on the plot can represent chemical reactions, such as (de)hydrogenation, (de)methylation, oxidation or reduction and others. Likewise, cross-plotting of H/C and corresponding *m/z* values disclose the molecular weight distribution of semi- and non-volatile compounds we detected in oven vapor. At this point, the chemical diversity of oven vapor becomes apparent: the detected features spread over a wide range of polarity and molecular mass. Further, one can visually perceive the impact of increased baking temperatures which leads to the previously discussed larger number of detected compounds and to compounds being present in different sections of the plots. Substance classes such as sugars, amino acids or fatty acids naturally settle into distinct regions in Van-Krevelen-plots as a matter of their molecular composition. All of the above named regions are well populated in samples from bread roll vapor. As data from FT-ICR-MS studies only permit assignment of molecular formulas to exact mass values, we performed further LC-MS/MS experiments to cover some of the annotations with concrete structures (see Supplementary Methods for details). Representative, non-volatile compounds for all of the substance classes named above, e.g., glucose, lysine and stearic acid were confirmed at level one (Sumner et al., 2007) to be present in our samples (see Supplementary Table 4 for further selected and identified compounds). Confirmation of single substances at level one is tedious and only feasible if standard substances are available. However, on one hand, the identifications provide evidence about the presence of semi- and non-volatile compounds in oven vapor. On the other hand, it allows us to demonstrate how the FT-ICR-MS serves as a powerful tool to quickly characterize the molecular fingerprinting of vapor samples. Through our holistic approach, the entity of the chemical system contained in the headspace is revealed and global response trends to altered processing conditions become apparent. Besides the naturally occurring molecular families named previously, Maillard reaction products (MRP) compose an important and well-studied compound class in cereal products which is induced by thermal treatment (Pozo-Bayón, Guichard, & Cayot, 2006). Consistently Rega et al. reported large quantities of several volatile MRPs to be present in oven vapor released from sponge cake (Rega et al., 2009). As recently shown, discrete compositional areas typical for MRP and caramelization products (CP) were identified based on Maillard model systems (Hemmler et al., 2018). We thrived to connect these findings towards the analysis of food samples. As the Maillard reaction (MR) initiates by the condensation of an amino acid with a carbohydrate, several starting points for the MR cascade on the Van-Krevelen canvas are given as a function of the molecular composition of the amino-moiety. In the course of the MR, intermediate species migrate towards lower H/C and O/C (respectively higher unsaturation) levels. Late stage MRPs such as heterocycles or melanoidins, finally settle towards the bottom left corner of the Van-Krevelen plot (Hemmler et al., 2018). We observed a magnitude of mass signals crowding distinct Maillard-related areas of the Van-Krevelen plot. Further we recognized a clear trend that application of higher baking temperatures pronounces MRP and CP areas at a higher density. Thus, we can confirm the findings of Rega et al. who described a major influence of the MR in oven vapor. As the MR is a reaction sequence enrolling from clearly non-volatile amino acids and carbohydrates, this finding exemplarily demonstrates how FT-ICR-MS analysis of oven vapor is crucial to gain insights about non-volatile compounds contained in this matrix. Another useful tool for the interpretation of ultra-high resolution mass spectra are Kendrick mass defect (KMD) plots. For KMD analysis, molecular building blocks, such as traditionally CH_2 in petroleomics, are converted to an integer value to

identify series of homologous species in complex organic mixtures (Kendrick, 1963; Kim et al., 2003). In an adapted KMD analysis we normalized the IUPAC mass of H_2O to a Kendrick mass scale (IUPAC mass × 18/18.010565). By plotting the Kendrick mass against the Kendrick mass defect of water, the dehydration series are projected onto horizontal lines (see Fig. 3f). In a vapor sample from bread rolls baked at 230 °C for 15 min we detected 37 of such series which show at least five incremental water transitions. These patterns reveal further traces of reaction cascades from (oligo)saccharides towards MRPs and CPs and can correspondingly be observed in studies on melanoidin formation and elucidations of Maillard model systems (Bruhns, Kanzler, Degenhardt, Koch, & Kroh, 2019; Hemmler et al., 2017). We detected dehydration cascades reaching up to a molecular mass of nearly 500 Da in our data set. Certainly FT-ICR-MS gives insight into heavier molecular spaces of oven vapor than accessible before through SPME–GC–MS and PTR-MS studies. For better readability, Van-Krevelen-plots with corresponding H/C to *m/z*-plots grouped into several compositional space can be found in Supplementary Fig. 2. As our baking processes took place in a humid atmosphere, we assume a complex system of transport reactions to take place between dough and its headspace, which are not only limited to the evaporation of hydrophobic volatiles. The presence of steam in the oven's headspace plays an important role and favors the transport of semi- and non-volatile molecules. When Rega et al. studied vapor from sponge cake baking by SPME–GC–MS, they explicitly mentioned the presence of the rather hydrophilic flavor compound 5-hydroxymethylfurfural (HMF) (Rega et al., 2009). Regarding the octanol/water partition coefficient, HMF has a log *P* value of –0.6 (all reported log *P* values according to XLogP3 3.0, PubChem release 2021.05.07). Our FT-ICR-MS analysis of oven vapor now unveils compounds with even higher polarity such as arginine (log $P = -4.2$) or maltose (log $P = -4.7$; both confirmed by LC–MS/MS, see Supplementary Material) to be present in oven vapor. Substances as these need to be transported towards the condensation apparatus by steam as they are not volatile themselves. Further, we confirmed the presence of palmitic and stearic acid (log $P = 6.4$ and 7.2 respectively) to be conveyed by vapor which demonstrates how FT-ICR-MS characterizes oven vapor over a wide range of analyte polarity. For the future, baking experiments with different steam settings are scheduled to investigate the relation between steam content of the oven atmosphere and the polarity of compounds contained in the headspace of a baking chamber. These findings depict a substantial extension of analyte polarity and molecular weight compared to species reported by SPME and PTR studies of oven vapor. In conclusion, we demonstrated how FT-ICR-MS validly characterizes the chemodiversity of oven vapor. It allows the following of global chemical trends triggered by food processing without losing focus in potentially misleading details.

3.3. Response surface analysis of molecules in oven vapor

Apart from characterizing the global composition of oven vapor, the scope of this study was to investigate the dynamic release of compounds during food processing to the oven headspace. Therefore, we sampled vapor from six bread rolls each baked at 21 different permutations of temperature and time (see Supplementary Table 2 for exact values). As we followed a cumulative vapor collection strategy, altered baking times in combination with modified baking temperatures yielded different quantities of trapped compounds during the experiments. By fitting second order polynomials to the variable feature intensities (see method section), we describe the features' signal intensity in oven vapor samples as a function of the processing parameters temperature and time. To perform reliable RSM calculations, we only considered features which were present in at least two out of three replicates of a vapor sample and in at least 15 out of 21 experimental temperature time combinations. We were able to calculate models for 991 features with an adjusted R^2 value > 0.6. Reflections upon response surface models of selected features in oven vapor permit us to follow the release of molecules during the cooking of foodstuff similar to Pico et al. who classified VOC based on the shape of their liberation curves during baking and toasting (Pico et al., 2020). Two easily interpretable examples are shown in Fig. 4. We first assessed the conduct of the feature annotated as $C_6H_{12}O_6$ (LC–MS/MS analysis identified glucose to be present in the vapor sample; see Supplementary Table 4). With rising baking temperature, we observed that the oven vapor contains a maximum of glucose, especially after longer processing times. A basic reaction in carbohydrate chemistry are dehydrations reactions. The initially formed hexose dehydration products are key intermediates in early phase Maillard and caramelization chemistry. We monitored this first dehydration product of glucose in oven vapor to demonstrate the traceability of an initial downstream reaction cascade (Fig. 4a). The dehydration products reach their maximum concentration during extensive and hot baking runs. Dividing the recorded intensity of the dehydration products by the one of glucose, the molar proportions become apparent which are lowest at 170 °C and come to a maximum at 224 °C. In the same way as we did for a monosaccharide, we monitored the conduct of the disaccharide maltose under the same conditions (Fig. 4b): at 170 °C a larger quantity of disaccharide was detected in oven vapor, the amount however diminishes with increasing temperature. The effect seems to be independent from the applied processing time. As maltose's relative concentration decreased, its dehydration products were complementarily formed, favorably under hot baking temperatures. A maximum ratio is reached at 242 °C. Initially formed carbohydrate dehydration products such as deoxyglucosones are known to be highly reactive compounds as their dicarbonyl structure is prone to nucleophilic attacks (Jost, Henning, Heymann, & Glomb, 2020). As our samples were cold trapped and frozen right after the baking process and our FT-ICR-MS system is capable of detecting ultra-traces of molecules through the accumulation of multiple scans per sample, we assume that we are able to detect a certain share of unreacted deoxyglucosones in the vapor. By direct comparison of both systems, we observed glucose to accumulate in vapor with higher baking temperature, whereas maltose simultaneously degrades. Recent results on quantitation of carbonyl compounds during industrial bread making processes indeed show that the concentration of glucose rises during baking as oligo- and polysaccharides are degraded to monosaccharides, first by enzymes and during later baking phases by thermal breakdowns. In contrast, after initial enzymatic reproduction of maltose, the major disaccharide in wheat bread, comes to an end, its concentration decreases from the pre-baking phase on with rising temperature, especially during late baking phases (Jost et al., 2020). Both processes are in agreement with our findings for the relative concentrations in the headspace of baked bread rolls. This demonstrates how FT-ICR-MS analysis of oven vapor can serve as a steam-assisted interface to the matrix. Non-volatile compounds released to the headspace of an oven reflect chemical reactions enrolling in the processed matrix. However, it should be noted that different isomers of an annotated molecular formula do not necessarily need to follow the same release pattern as they might be formed in different reaction pathways or even from different precursors. Keeping this bottle-neck in mind, we propose FT-ICR-MS as a sensitive tool for the at-line monitoring of chemical reactions in the underlying matrix.

Evaluation of our response surface models allows us to further understand the background of single molecular components, as the carbohydrates glucose and maltose demonstrate, within vapor as a part of the entire reactome of baked bread: we recognized at which conditions a compound reaches its maximum concentration in the headspace. Again, experiments for clarifying the release dynamics of non-volatiles to the oven headspace are to be performed to understand the underlying transport processes and the role of humidity in the system. The molecular modelling may help to optimize food production. On the one hand, enhancing the formation of compounds which mediate valued sensorial properties helps to increase the consumers' acceptance of a product. On the other hand, the formation of substances with a negative physiological background can be avoided. As oven vapor offers the possibility to

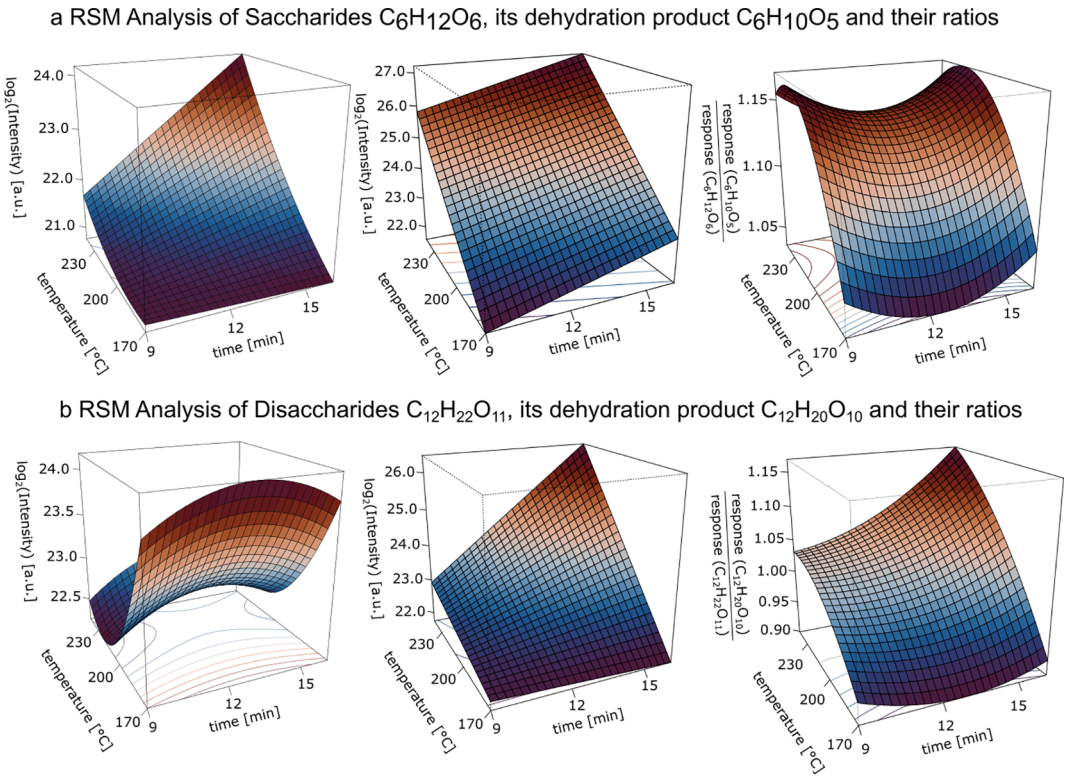

Fig. 4. 3-Dimensional plots showing the conduct of the mono- and disaccharide features, their dehydration products and their respective ratios in oven vapor resolved for different baking temperatures and times.

monitor compounds of interest directly in the headspace during the cooking process, extraction protocols for these compounds from the matrix after the baking process become obsolete and we see promising advances for online process supervision by the analysis of oven vapor.

3.4. *Tracking chemical reactions in oven vapor:*

As previously mentioned, we observed a substantial number of features related to the MR processes in our FT-ICR-MS screening of oven vapor. As early as in the 1950′s, Hodge et al. categorized the MR into three time-resolved phases of which the last phase describes the formation of compounds with high molecular weight, high degrees of aromaticity and unsaturation along with brown color (Hodge, 1953). This class of compounds is widely termed as advanced glycation end-products (AGE) and is currently under intense research by (bio) medical and food scientists (Goldberg et al., 2004; Hellwig, Kühn, & Henle, 2018; Kislinger et al., 1999; Ravichandran, Lakshmanan, Raju, Elangovan, Nambirajan, Devanesan, & Thilagar, 2019). In the previous section, we presented RSM models of compounds associable with early phase MR processes. However, FT-ICR-MS can follow complex reaction cascades from precursors *via* intermediates towards the formation of AGEs through accessing the information about non-volatile compounds contained in oven vapor. As an application of our oven vapor analysis in combination with response surface modelling, we describe in the following the formation of the AGE maltosine (6-(3-hydroxy-4-oxo-2-methyl-4(1*H*)-pyridin-1-yl)-l-norleucine). Maltosine develops in bread during baking by the addition of lysine to intermediately formed glucosyl isomaltol, a downstream product of maltose (Hellwig, Kiessling, Rother, & Henle, 2016). Fig. 5a visualizes the course of maltosine formation in our bread roll samples (230 °C, 15 min) through the

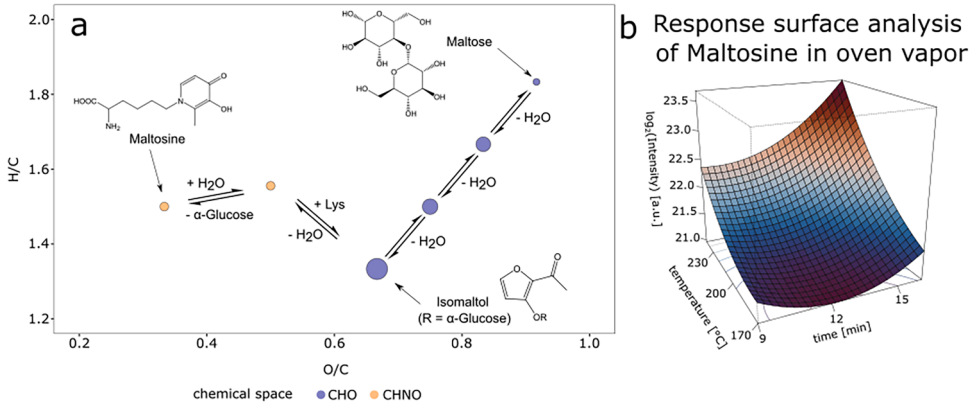

Fig. 5. **a** Traces of the Maillard reaction in oven vapor: the formation of maltosine from maltose and lysine (all identified by MS/MS, see Supplementary Materials and Methods, Supplementary Table 2 and Supplementary Fig. 3) can be followed over all intermediates (point size proportional to feature intensity). **b** Response surface analysis of maltosine in oven vapor from 21 different baking temperatures and durations.

interface of oven vapor in a Van-Krevelen-plot. It was shown that maltosine is an AGE evolving from disaccharides (Pischetsrieder & Severin, 2005), so we observed the initial series of dehydration reactions from maltose, which leads to the formation of glycosyl isomaltol, the most abundant feature in the reaction series. Followingly, condensation with lysine and cleavage of the glucose moiety leads to the formation of maltosine. We further monitored the evolution of maltosine by response surface modelling (Fig. 5b) as a function of baking temperature and time. During our baking experiments maltosine was formed at highest concentrations when baking at 230 °C for 15 min. Hellwig and co-workers showed that maltosine is predominantly formed in the bread crust up to 19.3 mg/kg (Hellwig et al., 2016). Therefore, it appears reasonable that the non-volatile maltosine is transported from the crust by steam during baking and collected in our sampling device. MRPs play an important role in various research disciplines, including flavor chemistry (Demyttenaere, Tehrani, & De Kimpe, 2002), food safety (Capuano, Ferrigno, Acampa, Ait-Ameur, & Fogliano, 2008) or biomedical research (Poulsen et al., 2013). Maltosine, for example, is known for its metal-chelating properties because of its 3-hydroxy-4-pyridinone structure (Geissler, Hellwig, Markwardt, Henle, & Brandsch, 2011). Further, as a covalent modification of the essential amino acid lysine, its formation alone reduces the biological value of food protein. Studies have shown that maltosine can modify up to 0.4% of lysine (Hellwig et al., 2016). Naturally, most of these modifications are covalently bound to larger peptides and proteins and, as a consequence, we would not expect their transport through steam. Nevertheless, the high sensitivity of the FT-ICR-MS screening not only can detect but also can actively follow the evolution of unbound maltosine through vapor without the need for extraction of the baked dough. In comparison to other oven vapor screenings discussed above, monitoring of entire reaction cascades is hardly feasible as both SPME–GC–MS and PTR-MS fail to detect the highly hydrophilic precursors of the reaction and are constrained to analyze volatile reaction end-products only.

3.5. Validation of RSM models:

The calculated models rely on measured feature intensities on a grid of pre-selected processing parameters. To verify that our models yield accurate response predictions, we randomly assigned two further VP within the studied factor ranges (VPI at 223 °C and 10 min, VPII at 180 °C and 14 min). We decided that the deviation between the validation records and respective model predictions must be of the same magnitude as the other model specific prediction errors. We calculated the standard deviation of the 63 datapoints' residuals (21 experimental factor combinations sampled as triplicates) for every model. In a following step we checked if the prediction by our RSM calculations ranged within two standard deviations from the value recorded under both validation conditions. We found 96% of all models to meet this criterion. Only 38 predictions were excluded as invalid by the validation experiments. Initially, we set high quality criteria for features to be selected for modelling based on replicate filtering and later only considered models with adjusted R^2 values > 0.6. Further we proved that based on carefully collected data, the prediction of relative concentrations of features in specified oven vapor systems is feasible. Thus, the transport of molecules from wheat bread rolls towards the oven headspace above underlies clearly structured and non-random processes which can be mathematically modelled and predicted.

4. Conclusion

By investigating trapped oven vapor arising from wheat bread roll baking with DIA-FT-ICR-MS, we showed that this matrix is a system rich in chemical information. Its chemodiversity reveals insights into the reactome that evolves during food processing with a focus on semi- and non-volatile compounds. Vapor-assisted transport processes give access to several thousands of compounds from the matrix over a broad range of molecular mass and polarity. Thus, our sampling strategy offers a promising perspective towards at-line sampling and consecutive analysis of cooking processes with a focus on semi- and non-volatile molecules. Besides a holistic description of the molecular entity, we used the contained chemical information for monitoring the evolving and depletion of selected features in the headspace of a professional oven under different processing parameters. Even the complex formation pathway of the AGE maltosine in bread rolls can be followed in oven vapor. Supplementary LC–MS/MS confirmed the identity of selected compounds throughout the entire reactome. We further showed response surface studies to be a useful tool to optimize baking conditions. In a consecutive step, we aim to compare the baked dough itself and its emitted vapor as well as the influence of the humidity content in the oven atmosphere on transport processes. This interlink shall help to understand the relations between new compounds formed in the food matrix and their liberation into the headspace. Altogether we see promising applications in analyzing oven vapor for semi- and non-volatile compounds in (bio-) medical, flavor and food sciences.

CRediT authorship contribution statement

Leopold Weidner: Conceptualization, Formal analysis, Investigation, Methodology, Software, Validation, Visualization, Writing – original draft, Writing – review & editing. **Yingfei Yan:** Methodology, Writing – review & editing. **Daniel Hemmler:** Conceptualization, Funding acquisition, Methodology, Project administration, Software, Writing – review & editing. **Michael Rychlik:** Resources, Supervision, Writing – review & editing. **Philippe Schmitt-Kopplin:** Conceptualization, Funding acquisition, Supervision, Project administration, Writing – review & editing.

Declaration of Competing Interest

The authors declare that they have no known competing financial interests or personal relationships that could have appeared to influence the work reported in this paper.

Acknowledgement

This work was funded by the Bavarian Ministry of Economic Affairs, Regional Development and Energy as a part of the BayVFP funding program - funding line digitalization - funding section information and communication technology.

Appendix A. Supplementary data

Supplementary data to this article can be found online at https://doi.org/10.1016/j.foodchem.2021.131618.

References

Ait Ameur, L., Rega, B., Giampaoli, P., Trystram, G., & Birlouez-Aragon, I. (2008). The fate of furfurals and other volatile markers during the baking process of a model cookie. *Food Chemistry, 111*(3), 758–763. https://doi.org/10.1016/j.foodchem.2007.12.062

Akaike, H. (1974). A new look at the statistical model identification. *IEEE Transactions on Automatic Control, 19*(6), 716–723. https://doi.org/10.1109/TAC.1974.1100705

Bruhns, P., Kanzler, C., Degenhardt, A. G., Koch, T. J., & Kroh, L. W. (2019). Basic structure of melanoidins formed in the maillard reaction of 3-deoxyglucosone and γ-aminobutyric acid. *Journal of Agricultural and Food Chemistry, 67*(18), 5197–5203. https://doi.org/10.1021/acs.jafc.9b00202

Capuano, E., Ferrigno, A., Acampa, I., Ait-Ameur, L., & Fogliano, V. (2008). Characterization of the Maillard reaction in bread crisps. *European Food Research and Technology, 228*(2), 311–319. https://doi.org/10.1007/s00217-008-0936-5

Demyttenaere, J., Tehrani, K. A., & De Kimpe, N. (2002). The chemistry of the most important maillard flavor compounds of bread and cooked rice. *ACS Symposium Series, 826*(Figure 1), 150–165.

Geissler, S., Hellwig, M., Markwardt, F., Henle, T., & Brandsch, M. (2011). Synthesis and intestinal transport of the iron chelator maltosine in free and dipeptide form.

European Journal of Pharmaceutics and Biopharmaceutics, 78(1), 75–82. https://doi.org/10.1016/j.ejpb.2010.12.032

Goldberg, T., Cai, W., Peppa, M., Dardaine, V., Baliga, B. S., Uribarri, J., & Vlassara, H. (2004). Advanced glycoxidation end products in commonly consumed foods. *Journal of the American Dietetic Association, 104*(8), 1287–1291. https://doi.org/10.1016/j.jada.2004.05.214

Hellwig, M., Kiessling, M., Rother, S., & Henle, T. (2016). Quantification of the glycation compound (maltosine) in model systems and food samples. *European Food Research and Technology, 242*(4), 547–557. https://doi.org/10.1007/s00217-015-2565-0

Hellwig, M., Kühn, L., & Henle, T. (2018). Journal of Food Composition and Analysis Individual Maillard reaction products as indicators of heat treatment of pasta — A survey of commercial products. *Journal of Food Composition and Analysis, 72*(March), 83–92. https://doi.org/10.1016/j.jfca.2018.06.009

Hemmler, D., Roullier-Gall, C., Marshall, J. W., Rychlik, M., Taylor, A. J., & Schmitt-Kopplin, P. (2017). Evolution of complex Maillard chemical reactions, resolved in time. *Scientific Reports, 7*(1), 3–8. https://doi.org/10.1038/s41598-017-03691-z

Hemmler, D., Roullier-Gall, C., Marshall, J. W., Rychlik, M., Taylor, A. J., & Schmitt-Kopplin, P. (2018). Insights into the chemistry of non-enzymatic browning reactions in different ribose-amino acid model systems. *Scientific Reports, 8*(1), 1–12. https://doi.org/10.1038/s41598-018-34335-5

Hertkorn, N., Frommberger, M., Witt, M., Koch, B. P., Schmitt-Kopplin, P., & Perdue, E. M. (2008). Natural organic matter and the event horizon of mass spectrometry. *Analytical Chemistry, 80*(23), 8908–8919. https://doi.org/10.1021/ac800464g

Hodge, J. E. (1953). Dehydrated foods, chemistry of browning reactions in model systems. *Journal of Agricultural and Food Chemistry, 1*(15), 928–943. https://doi.org/10.1021/jf60015a004

Jost, T., Henning, C., Heymann, T., & Glomb, M. A. (2020). Comprehensive analyses of carbohydrates, 1,2-dicarbonyl compounds and advanced glycation endproducts in industrial bread making. *Journal of Agricultural and Food Chemistry, 69*(12), 3720–3731. https://doi.org/10.1021/acs.jafc.0c07614

Kanawati, B., Bader, T. M., Wanczek, K. P., Li, Y., & Schmitt-Kopplin, P. (2017). Fourier transform (FT)-artifacts and power-function resolution filter in Fourier transform mass spectrometry. *Rapid Communications in Mass Spectrometry, 31*(19), 1607–1615. https://doi.org/10.1002/rcm.7940

Kendrick, E. (1963). A mass scale based on CH2 = 14.0000 for high resolution mass spectrometry of organic compounds. *Analytical Chemistry, 35*(13), 2146–2154. https://doi.org/10.1021/ac60206a048

Kim, S., Kramer, R. W., & Hatcher, P. G. (2003). Graphical method for analysis of ultrahigh-resolution broadband mass spectra of natural organic matter, the Van Krevelen diagram. *Analytical Chemistry, 75*(20), 5336–5344. https://doi.org/10.1021/ac034415p

Kislinger, T., Fu, C., Huber, B., Qu, W., Taguchi, A., Yan, S. D., … Pischetsrieder, M. (1999). N(ε)-(carboxymethyl)lysine adducts of proteins are ligands for receptor for advanced glycation end products that activate cell signaling pathways and modulate gene expression. *Journal of Biological Chemistry, 274*(44), 31740–31749. https://doi.org/10.1074/jbc.274.44.31740

Lee, C. C., & Chen, C.-H. (1966). Studies with Radioactive Tracers IX. The Fate of Sucrose-14C during Breadmaking. *In Cereals and Grains Association*.

Marshall, A. G., Hendrickson, C. L., & Jackson, G. S. (1998). Fourier transform ion cyclotron resonance mass spectrometry: a primer. *Mass Spectrometry Reviews, 17*(1), 1–35. https://doi.org/10.1002/(SICI)1098-2787(1998)17:1<1::AID-MAS1>3.0.CO;2-K

Marshall, A. G., & Rodgers, R. P. (2004). Petroleomics: the next grand challenge for chemical analysis. *Accounts of Chemical Research, 37*(1), 53–59. https://doi.org/10.1021/ar020177t

Pence, E.A. (1952). *A Study of baking oven vapors*. Kansas State University of Agriculture and Applied Science.

Pico, J., Khomenko, I., Capozzi, V., Navarini, L., & Biasioli, F. (2020). Real-time monitoring of volatile compounds losses in the oven during baking and toasting of gluten-free bread doughs: A PTR-MS evidence. *Foods, 9*(10), 1498. https://doi.org/10.3390/foods9101498

Pieczonka, S. A., Lucio, M., Rychlik, M., & Schmitt-Kopplin, P. (2020). Decomposing the molecular complexity of brewing. *NPJ Science of Food, 4*(1), 1–10. https://doi.org/10.1038/s41538-020-00070-3

Pischetsrieder, M., & Severin, T. (2005). In *Maillard Reactions in Chemistry, Food and Health* (pp. 37–42). Elsevier. https://doi.org/10.1533/9781845698393.2.37.

Poulsen, M. W., Hedegaard, R. V., Andersen, J. M., de Courten, B., Bügel, S., Nielsen, J., … Dragsted, L. O. (2013). Advanced glycation endproducts in food and their effects on health. *Food and Chemical Toxicology, 60*, 10–37. https://doi.org/10.1016/j.fct.2013.06.052

Pozo-Bayón, M. A., Guichard, E., & Cayot, N. (2006). Flavor control in baked cereal products. *Food Reviews International, 22*(4), 335–379. https://doi.org/10.1080/87559120600864829

Ravichandran, G., Lakshmanan, D. K., Raju, K., Elangovan, A., Nambirajan, G., Devanesan, A. A., & Thilagar, S. (2019). Food advanced glycation end products as potential endocrine disruptors: An emerging threat to contemporary and future generation. *Environment International*, *123*(December 2018), 486–500. https://doi.org/10.1016/j.envint.2018.12.032.

Rega, B., Guerard, A., Delarue, J., Maire, M., & Giampaoli, P. (2009). On-line dynamic HS-SPME for monitoring endogenous aroma compounds released during the baking of a model cake. *Food Chemistry, 112*(1), 9–17. https://doi.org/10.1016/j.foodchem.2008.05.028

Rochat, S., & Chaintreau, A. (2005). Carbonyl odorants contributing to the in-oven roast beef top note. *Journal of Agricultural and Food Chemistry, 53*(24), 9578–9585. https://doi.org/10.1021/jf058089l

Roullier-Gall, C., Boutegrabet, L., Gougeon, R. D., & Schmitt-Kopplin, P. (2014). A grape and wine chemodiversity comparison of different appellations in Burgundy: Vintage vs terroir effects. *Food Chemistry, 152*, 100–107. https://doi.org/10.1016/j.foodchem.2013.11.056

Roullier-Gall, C., Signoret, J., Hemmler, D., Witting, M. A., Kanawati, B., Schäfer, B., … Schmitt-Kopplin, P. (2018). Usage of FT-ICR-MS metabolomics for characterizing the chemical signatures of barrel-aged whisky. *Frontiers in Chemistry, 6*(2), 1–11. https://doi.org/10.3389/fchem.2018.00029

Stekhoven, D. J., & Bühlmann, P. (2012). Missforest-Non-parametric missing value imputation for mixed-type data. *Bioinformatics, 28*(1), 112–118. https://doi.org/10.1093/bioinformatics/btr597

Sumner, L. W., Amberg, A., Barrett, D., Beale, M. H., Beger, R., Daykin, C. A., … Viant, M. R. (2007). Proposed minimum reporting standards for chemical analysis: Chemical Analysis Working Group (CAWG) Metabolomics Standards Initiative (MSI). *Metabolomics, 3*(3), 211–221. https://doi.org/10.1007/s11306-007-0082-2

Tziotis, D., Hertkorn, N., & Schmitt-Kopplin, P. (2011). Kendrick-analogous network visualisation of ion cyclotron resonance Fourier transform mass spectra: Improved options for the assignment of elemental compositions and the classification of organic molecular complexity. *European Journal of Mass Spectrometry, 17*(4), 415–421. https://doi.org/10.1255/ejms.1135

Wieland, F., Gloess, A. N., Keller, M., Wetzel, A., Schenker, S., & Yeretzian, C. (2012). Online monitoring of coffee roasting by proton transfer reaction time-of-flight mass spectrometry (PTR-ToF-MS): Towards a real-time process control for a consistent roast profile. *Analytical and Bioanalytical Chemistry, 402*(8), 2531–2543. https://doi.org/10.1007/s00216-011-5401-9